Measuring the Electronic Properties of Thin-Film TiO$_2$ Polymorphs

Kelda Diffendaffer

Adviser: Dr. Janet Tate

Oregon State University, Physics Department

5/23/2019

1   Abstract

There are many factors that affect the resistivity of a TiO$_2$ thin film, but the most important one is the presence or absence of oxygen vacancies, which is controllable through the partial pressure of oxygen during sputter coating. To accurately measure TiO$_2$'s electrical properties (such as its Hall coefficient, carrier type, carrier density, etc), we must have a resistivity below 400 mohm cm. This will occur when the TiO$_2$ is underoxygenated, or TiO$_{2-x}$. Brookite is especially difficult to measure, as underoxygenated brookite easily becomes rutile instead. Further study is necessary to determine how to make underoxygenated and pure brookite.

Contents

2   Introduction

TiO_2 is a simple oxide system, with three common metastable polymorphs: rutile, anatase, and brookite. The conditions that lead to the synthesis of one polymorph over another are mysterious, particularly in the case of

brookite. Previous research by this group [1][2] indicates that the amount of oxygen present during the synthesis conditions strongly affects which polymorph is formed, with rutile being formed with thicker films with less oxygen, while anatase is formed with more oxygen (with brookite forming somewhere around the middle). However, using oxygen to select for a polymorph leads to challenges in determining the electrical properties of the polymorphs.

When stoichometrically pure, TiO_2 is an electrical insulator, with strong bonds and no carrier motion of any kind. However, TiO_{2-x} is generally an n-type semiconductor [3], which means that electrons are the majority charge carriers. Oxygen vacancies are the cause of these extra electrons in the conduction band, and the more oxygen vacancies a sample of TiO_2 has, in general, the more conductive we expect the material to be. Adequate conductivity is vital for accurate measurements of the electrical properties of the materials.

To measure the electrical properties of the material, we need to isolate the effect that the polymorph has on the resistivity, carrier concentration, Hall coefficient, etc. In this thesis, I will attempt to isolate the effect that specific polymorphs have on the electrical properties of a thin film of TiO_{2-x}. I will also detail the other factors that must be accounted for when measuring a thin film of TiO_{2-x} and their expected effects, in the hopes that further research will be able to effectively determine the effect of specific polymorphs on the electrical properties of TiO_2. For the method of polymorph selection through oxygen levels present during deposition to be successful - not just for TiO_2, but other oxide systems as well - this must be well understood.
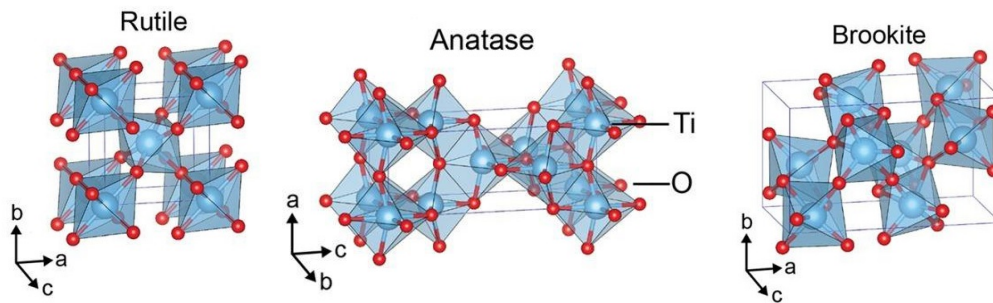
Figure 1: ~~Crystallography~~ *Polymorphs* of TiO$_2$. Brookite is easily distinguishable from rutile and anatase. In this model, blue atoms are titanium, and red are oxygen. [1]

2.1 The TiO$_2$ Polymorph System

TiO$_2$ is a useful material, with applications including pigments, semiconductors, reflective coatings for dielectric mirrors, and, most interesting to researchers, as a photocatalyst. Nanosized titanium dioxide (both in a thin film and a nanoparticle form) acts as a catalyst for a reaction that absorbs UV light and, in the case of TiO$_2$, generates free radicals which oxidize the target material. This phenomenon can be used for many self-cleaning, sterilizing, hydrophobic, deodorizing, anti-fouling, anti-fogging, and pollution reducing coatings [4]. However, photocatalytic activity is not equally present among the polymorphs of TiO$_2$.

There are three relatively stable forms of TiO$_2$: rutile (tetragonal), anatase (tetragonal) and brookite (orthorhombic). See figure 1 for more details. At all temperatures and pressures, anatase is less stable than rutile, and brookite is even more unstable [5]. While antase and brookite are metastable, when heated to around 600° C, anatase converts to rutile irreversibly. Brookite is even more unstable than anatase. Over the last few decades, thin films
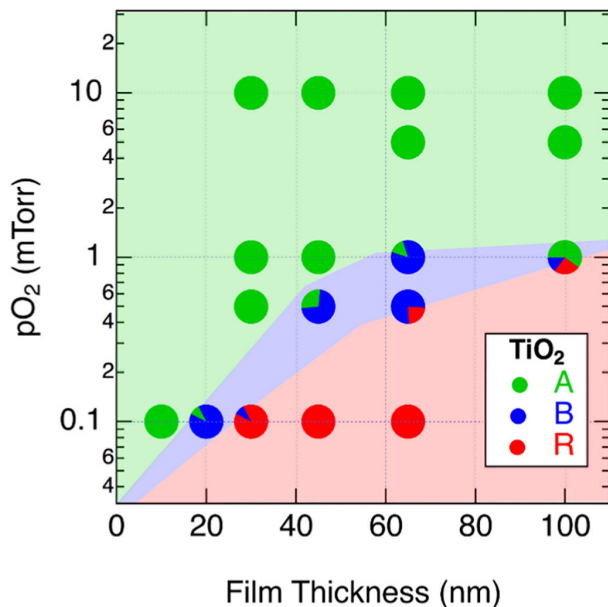
Figure 2: Visualization of the relationship between thickness, oxygen pressure (pO_2) during deposition, and the TiO_2 polymorphs formed after annealing at $400°$ C. The location of the circles indicates film thickness and pO_2 during deposition, while the coloring indicates the fraction of each polymorph formed after crystallization. Red indicates rutile; green indicates anatase and blue indicates brookite. [2]

of mixes of polymorphs including brookite have been produced but until recently, few pure thin films could be produced to study. Most of the techniques for creating thin films result in anatase. Takahashi et al. were among the first to prepare almost pure brookite films with vapor phase decomposition of tert-butyl titanate [6]. Since then, many have synthesized brookite with methods ranging from PVD (physical vapor deposition) to hydrothermal syntheses. However, while many have had success in producing brookite films, the mechanism for stabilization of this metastable polymorph is unclear.

In 1956, Mashio et al. published a paper on the photocatalytic behavior of TiO_2. They concluded that, in nanoparticle form, anatase was the most ef-

ficient photocatalytic form of TiO_2 [4]. However, later research showed that the inclusion of brookite in samples of antase boosted the photocatalytic effect of the material [4]. Nanocrystalline brookite particles have been analyzed and found to be comparable and perhaps superior to nanocrystalline anatase as a photocatalyst. Research into brookite-rich thin films is rarer, but brookite-rich thin films were found to behave in ways largely consistent with better performance as a photocatalyst than anatase films [6].

Brookite is therefore an understudied and promising material, but it has proven difficult to synthesize. A paper published by the Tate group earlier this year sheds light on why - see figure 2. Brookite forms reliably only in a narrow range of parameters. This presents additional problems for control of oxygen vacancies - too much or too little oxygen during synthesis can easily cause rutile or anatase to form instead of brookite, or for a mixture to form (which presents uniformity problems during measurement)[2]. Ideally, we would like to be able to synthesize pure brookite thin films with the amount of oxygen vacancies that we desire.

2.2 Electrical Properties Relation to Thin Film Synthesis

Stoichiometric TiO_2 is an electrical insulator when in crystalline form. Titanium bonds with the oxygens strongly, and this results in no carrier motion between atoms. TiO_{2-x} is deficient in oxygen, and thus the titanium atom has extra electrons in its conduction band, from the unsatisfied bonds previously filled by oxygen. These electrons are available to be carriers, and

transfer from titanium atom to titanium atom, in search of a hospitable location. The more oxygen defects a given polymorph has, the more we would expect it to conduct.

The predominant defects in high purity single-crystal TiO_2 have been determined to be oxygen vacancies [3]. (Interestingly, however, very oxidized TiO_{2+x} pure crystals display p-type behavior. We did not observe this, nor would we expect to, as this occurs only in extremely oxidized samples [3][7]. Technically, TiO_2 is an amphoteric semiconductor, but we will only consider n-type situations.) The conductivity of TiO_2 can be tuned by controlling these vacancies, and this has been done in a variety of other forms such as nanowires and resistive switching devices [8][9].

Besides the oxygen vacancies, there are other factors that affect the resistivity of the material: phases, grain boundaries, and the overall crystallinity. We believe that the phase of the TiO_2 (rutile, anatase, or brookite) matters to the conductivity of the thin film, but data on this is difficult to find, especially isolated from other effects on conductivity. It is difficult to make high quality, pure thin films of specific polymorphs, so there is a second effect we need to consider when determining their electrical properties, which is the geometries of mixed phase samples. Chunks of an unwanted phase could disrupt the flow of current within the sample. Amorphous samples, on the other hand, will not have much in the way of crystal grain boundries as compared to a fully crystallized mixed-phase sample. Within grains however, better crystallinity increases the mean free path which means a decreased resistivity.

2.3 Electrical Properties: What to Measure

The simplest electrical property we can measure is the resistivity (ρ). We put current through the sample and measure its resistance, then compensate for the geometry of our sample and various errors that may occur due to imperfections in the material. The resistivity measured is a fundamental property of the material and not dependent on the size and shape of the sample.

The three most interesting and useful electrical properties of a material are the carrier density, mobility, and the carrier type, all of which are more difficult to measure. Carriers can be of two types (or a mix of the two): electrons or electron holes. These correspond to p and n type semiconductors respectively. Carrier density refers to the number of carriers per a unit of volume, and the mobility refers to how easily the carriers move through the material. The more carriers are available to carry charge or the higher the mobility, the more conductive the material is. Determining these values is not as simple as determining resistivity, and we must apply something called the Hall effect to this problem. See figure 3.

When a magnetic field is applied perpendicularly to an electric field, the magnetic field exerts a force on the carriers and pushes them in a direction that is dependent on the type of carrier the material has. This is known as the Hall effect, which is really based on the Lorentz force. When an electron moves in the direction of the current flow, it experiences a force (F_m):

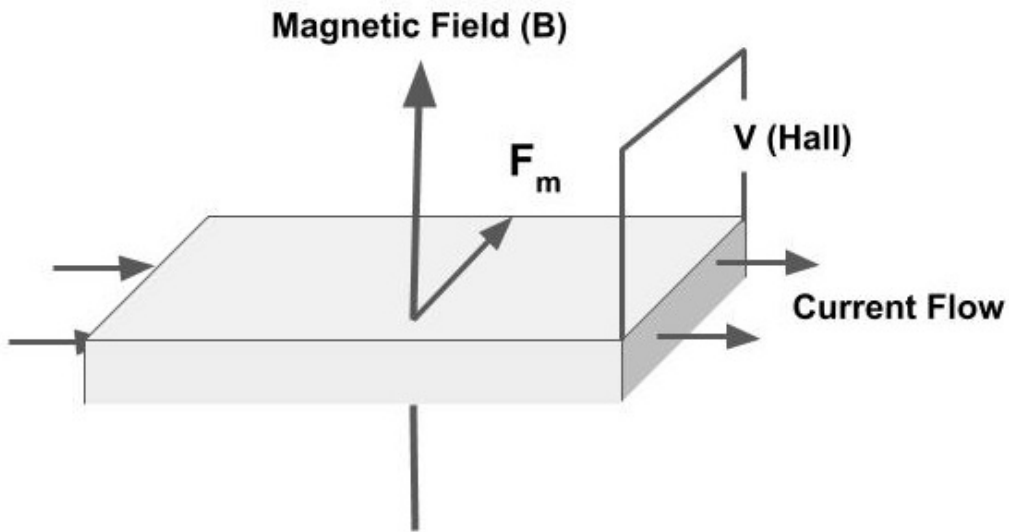$$\vec{F_m} = -q\vec{v_d} \times \vec{B} \tag{1}$$

Figure 3: Diagram of the Hall Effect. The magnetic field, applied perpendicularly to the current flow, causes a voltage, due to the Lorentz force pushing carriers either with or against the arrow labeled F_m.

Where $\vec{v_d}$ is the drift velocity of the carrier [10]. Pushed by this force, charge carriers are pushed to the edge of the sample. If the charge carriers are holes, there will be a build up of positive charge pushed in the direction of $\vec{F_m}$, and corresponding negative charge will build up on the opposite edge. If the charge carriers are electrons, the build up of charge will be negative, and the resulting Hall voltage will be opposite in sign, when compared to the case with holes as the charge carriers. Some additional mathematics allows us to relate the sign and magnitude of the Hall voltage to the charge density, carrier type, and the mobility.

With these values, we know a great deal about the nature of the material we are measuring.
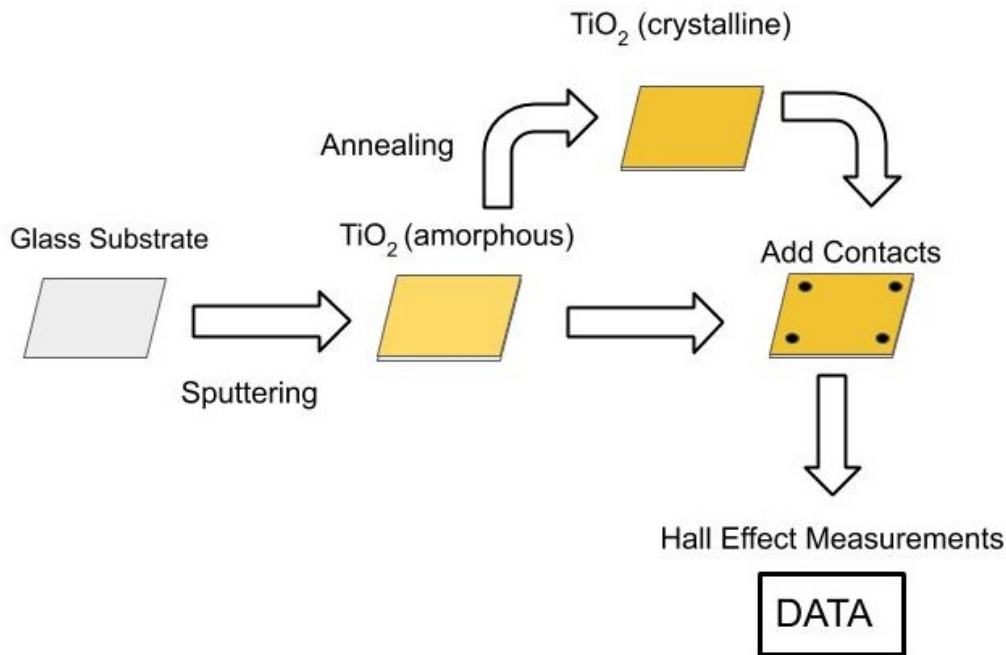
Figure 4: A summary of the production and measurement process. Alternate methods of deposition are possible, and amorphous samples are measured the same way as crystalline TiO₂ samples are.

3   Methods

The data-gathering process can divided up into 5 steps: synthesis of amorphous samples, conversion to crystalline forms, preparation for measurement, measurement, and analysis. An overview of the process is shown in figure 4.

3.1   Synthesis

Samples consist of a thin film (15 - 60 nm) of TiO_2 on glass (a-SiO2, GM associates).These are produced via RF sputter deposition, which provides good uniformity, smoothness, and highly controllable thickness. Sputtering

is a high energy deposition technique which uses molecules of an inert gas (argon in this instance) to transfer energy to a target of material, removing particles of the material (in our case titanium). Ionized argon strikes the titanium metal target, pulled in by a RF voltage applied between the target and the substrate. The ejected titanium particles fly off from the target in every direction, coating the inside of the chamber, and thereby the sample, with titanium. These particles often retain a high mobility when they strike the substrate, leading to an increase in crystallinity in the sample (increasing the structure in our 'amorphous' films). The presence of oxygen gas in the system causes us to deposit an oxide of titanium, rather than pure titanium. This coating varies from completely transparent to a dark and shiny gold color (see figure 5).

After cleaving into an appropriate size (about 1 cm^2), these 'amorphous' samples can be prepared for measurement, but to compare the amorphous precursor films to the crystalline results, half of each sample is rapidly annealed (using an AET Thermal RX thermal annealer) in flowing nitrogen at 400 °C for varying lengths of time. These samples are then cleaved as well, and prepared for measurement.

It is important to note that, during synthesis, the partial pressure of oxygen is varied to provide a rough control of x, in the formula TiO$_{2-x}$. Lower pO2 corresponds to higher x, and higher pO2 corresponds to lower x. Additionally, during annealing, oxygen content was intended to be held constant, but the nitrogen flush is imperfect, and can allow some oxygen to be added to the sample.
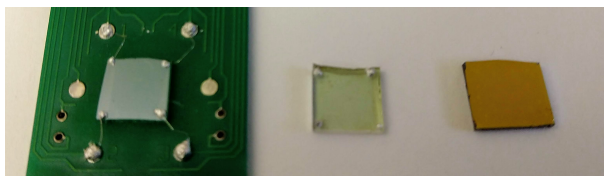
Figure 5: Samples of TiO_2, from left to right: 1 - Sample mounted onto sample board, 2 - sample with contacts attached, and 3- a cleaved but untouched sample. The third sample's color is indicative of a highly conductive rutile sample, while the other two are nearly clear, and are likely to have a lower conductivity.

3.2 Preparation for Measurement

Our samples are measured two primary ways: optically and electrically. While thickness can be estimated based on synthesis conditions, thickness is verified optically by measuring reflectance and transmittance, then analyzed with LabSpec 5.0 and SCOUT. Thickness can also be verified with EPMA profilometers. Raman spectroscopy (Horiba Jobin-Yvon LabRam800) is the primary tool for determining the phase of the material.

To accurately measure electrical properties, we must make indium contacts on the thin film. This is done with a soldering iron set at 230 °C. A dab of pure indium solder is melted to the contact pads on the measurement card, which simply allows us to measure between contact points swiftly and accurately. Another dab of indium solder is added to the sample. On the film itself, our contacts must be very small, around 20 microns in our case, as close to the edges of our sample as possible, and equidistant from each other. A nickel chromium wire (Tophet A), is then used to attach the indium contacts to contact pads on measurement boards for the Lakeshore 7504 Hall Measurement System (HMS).

Using the Lakeshore Hall system, we pass current through the material and measure the resultant voltage accurately, while varying the magnetic field. This allows us to calculate the resistivity of the material, doping type, sheet carrier density and the carrier mobility. Given the imperfect shape of our sample, a rough rectangle, we apply van der Pauw's method. This method has four conditions: the contacts are at the circumference of the sample, the contacts are sufficiently small, the sample is homogeneous in thickness, and the surface does not contain isolated holes [10]. Error is introduced by large contacts on the order of D/L, where D is the average diameter of the contact and L is the distance between them, so just from our minimized contact size ($D = 20\ \mu$ m, $\ L = 1$ cm), we can expect error on the order of 0.2.

3.3 Measurement

We use a Lakeshore 7504 Hall Measurement System (HMS). It is capable of measuring the Hall coefficient, carrier density, and resistivity of the material. It consists of an electromagnet (which produces up to 8.0 kG in its current configuration), a constant-current source (Kiethley 220 Programmable Current Source with a Kiethley 465 Autoranging Picoammeter for accuracy), a high input impedance nanovoltmeter (Keithley 2182 Nanovoltmeter), and software to compute properties of the material from simple measurements.

Four leads are connected to four contacts which fit van der Pauw's criteria, see figure 6. They must be considerably smaller than the sample length, equidistant from each other, close to edge but not touching it, and the contact
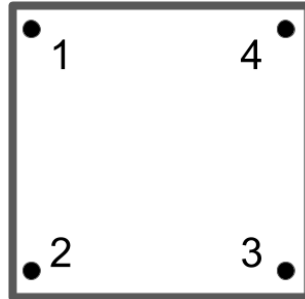
Figure 6: Contact Placement on Sample.

must be ohmic.

This allows us to pass a constant current in through any two points we choose, and to measure the resulting voltage through two other contacts. By applying van der Waal's formula and then the mathematics necessary to determine the Hall coefficient, we can determine various properties of the material.

We first need to define several parameters:

- ρ = sample resistivity (in Ω cm)

- d = conducting layer thickness (in cm)

- I_{12} = positive DC current I injected into contact 1 and taken out of contact 2. Likewise for I_{23}, I_{34}, etc.

- V_{12} = DC voltage measured between contacts 1 and 2 ($V_1 - V_2$). Likewise for V_{23}, V_{34}, etc.

Ideally, the sample will be internally consistent (ie single phase or amorphous), totally uniform, and with completely ohmic contacts. This is never
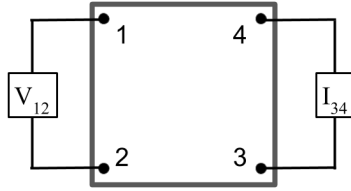
14

Figure 7: Four terminal resistance, shown with an applied current $I_{3,4}$ and a measured voltage of $V_{1,2}$.

the case, so we check for consistency by measuring the material with different geometries. The procedures followed are detailed by NIST [11], and seem complex but arise from a simple concept: given a uniform material, the orientation of the measurement with respect to the sample should not matter. Therefore, we can obtain more accurate data by measuring the sample with the current and field reversed, or from opposite contacts. Any constant offset in the voltage measured will not reverse with the change in orientation, and can be identified through this. There are many ways that errors in the voltage measured can creep in. For instance, a temperature gradient in the material will introduce a Seebeck voltage, so temperature must be stabilized.

3.3.1 Resistivity

Measuring the resistivity of the material does not require a magnetic field, though including the effects of a magnetic field will inform us if it is a magnetoresistive material. First, we measure four-terminal resistance (see figure 7) for all possible orientations, given that the terminals we measure voltage from cannot be the same as the terminals we put current into (excluding diagonal connections, like V_{13}).

This gives us eight measurements of voltages, which corresponds to eight values of resistances:

$$R_{21,34} = V_{34}/I_{21} \tag{2}$$

Once the resistance has been calculated with each geometry, we can calculate the characteristic resistances.

$$R_A = (R_{21,34} + R_{12,43} + R_{43,12} + R_{34,21})/4 \tag{3}$$

$$R_B = (R_{32,41} + R_{23,14} + R_{14,23} + R_{41,32})/4 \tag{4}$$

These characteristic resistances can be used to calculate the sheet resistance (R_s) by applying the van der Pauw equation:

$$e^{(-\pi*R_A/R_S)} + e^{(-\pi R_B/R_S)} = 1 \tag{5}$$

A numerical solution to this equation is used, and all calculations are automatically performed by the Lakeshore HMS software. Using the optical measurements for the thickness (or our estimates based on highly predictable deposition rates), we can calculate the bulk resistivity:

$$\rho = R_s d \tag{6}$$

This is independent of the sample geometry and size, and is an important property of the material itself.
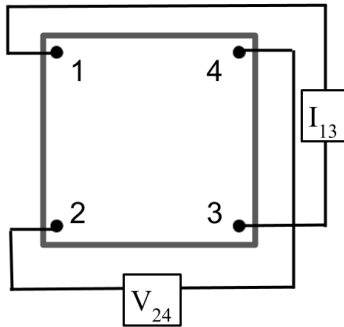
16

Figure 8: Example of four terminal resistance, for hall effect measurements.

3.3.2 Hall Measurements

Unlike the resistivity measurements, the Hall measurements require a strong, precise and controllable magnetic field. As described earlier, the Hall voltage arises from the application of a magnetic field perpendicular to the flow of current. To explain the procedure, we must define new terms:

- B = a constant and uniform magnetic field intensity, applied parallel to the z-axis (so, the magnets are parallel to the surface of the sample). B is positive when the field points in the positive z direction, and negative when it points in the negative z direction. B must be uniform and constant within 3% and within a few degrees of exactly parallel for our data to be accurate.

- d = conducting layer thickness (in cm)

- $V_{12,-B}$ = Hall voltage, measured between terminals 1 and 2 with a negative magnetic field. Likewise for V_{23N}, $V_{34,-B}$, etc.

- $V_{12,+B}$ = Hall voltage, measured between terminals 1 and 2 with a

positive (P) magnetic field. Likewise for $V_{23,+B}$, $V_{34,+B}$, etc.

First, we apply a positive magnetic field, B. We apply a current diagonally across the sample (see figure 8) and measure the voltage across the two remaining terminals (for example, inputting I_{13} and measuring $V_{24,+B}$). We then flip the current's direction (from I_{13} to I_{31}, for example), and measure the Hall voltage again, from the opposite direction (from $V_{24,+B}$ to $V_{42,+B}$). We then flip the locations of the input and output terminals, and repeat the measurements. Finally, we repeat the process with the field direction flipped.

This results in eight measurements of Hall voltages, which can be used to determine the sample type (n or p) and the sheet carrier density n_s. The carrier type determines the sign of the Hall voltage (depending on if the charge carriers are electron holes or electrons), and the carrier density determines the magnitude of the Hall voltage. The more charge carriers there are, the stronger the Hall effect is.

The sample type is determined by the sign of V_{all}, with positive being p-type and negative being n-type.

$$V_{all} = V_C + V_D + V_E + V_F \tag{7}$$

$$V_C = V_{24,+B} - V_{24,-B} \tag{8}$$

$$V_D = V_{42,+B} - V_{42,-B} \tag{9}$$

$$V_E = V_{13,+B} - V_{13,-B} \tag{10}$$

$$V_F = V_{31,+B} - V_{31,-B} \tag{11}$$

18

The sheet carrier density (in cm^{-2}) is calculated for p-type with:

$$p_s = 8 * 10^{-8} \frac{IB}{qV_{all}} \tag{12}$$

And for n-type:

$$n_s = |8 * 10^{-8} \frac{IB}{qV_{all}}| \tag{13}$$

Where I is the input dc current in amperes. Specify units of q, V, B

The bulk carrier density (in cm^{-3}) can be calculated from the sheet carrier density, if we know the thickness of the conducting layer.

$$n = \frac{n_s}{d} \tag{14}$$

$$p = \frac{p_s}{d} \tag{15}$$

Finally, we can calculate μ, the Hall mobility (in cm$^2 volts^{-1} sec^{-1}$).

$$\mu = \frac{1}{qn_s R_s} \tag{16}$$

This requires us to know the sheet resistance, which we determined earlier with resistivity.

4 Results

4.1 Electrical

Thirty nine samples were measured, but resistivity was measurable for only eighteen. Of those eighteen, only eight had a high enough signal for the Hall effect measurements that those were measurable (that is, enough carriers that the effect of the magnetic field would be measurable). See figure 9 for these fully measurable samples.

More samples were measurable for just resistivity. These are included in figure 10.

TiO2		pO2 (%)	Time (min)	Predicted Thickness (nm)	Resistivity (@5kG)	Carrier Density (cm^3/C)	Visual	Brookite	Rutile	Anatase
S-005	Post	4.26	30	60	393 μohm cm	0.7*10^24	Dark Gold	0	100	0
S-005	Pre	4.26	30	60	16.22 ohm cm	0.25*10^19		0	100	0
S-011	Post	2.86	15	30	315.75 mohm cm	0.7*10^20	Clear	60	40	0
S-011	Pre	2.86	15	30	3.915 ohm cm	0.65*10^19		60	40	0
S-017	Post	0.43	7.5	15	332 mohm cm	0.4*10^20	Silver	0	2	98
S-017	Pre	0.43	7.5	15	1.0425 mohm cm	0.53*10^23		0	2	98
S-025	Post	2.86	17	34	9.21 ohm cm	0.7*10^18	Clear	99	1	0
S-049	Post	2.86	20	40	147.4 mohm cm	1*10^20		97	3	0
S-039	Pre	2.86	52	104	4.03 ohm cm	0.2*10^19		Low	High	None

Figure 9: Successfully measured samples, including Hall data. Predicted thickness is based on deposition rates, and has proven to be within a few nm of the optically measured thickness. Polymorph percentages are an estimate, based on optical measurements.

4.2 EPMA

Electron probe microanalysis (or EMPA) is a measurement technique which uses a powerful electron source to bombard the material to be analyzed, which liberates matter and energy from the sample. X-rays in particular are emitted in various ranges characteristic of the elemental species present

TiO2		pO2 (%)	Time (min)	Predicted Thickness (nm)	Resistivity (@5kG)	Visual	Brookite	Rutile	Anatase
S-005	Post	4.26	30	60	393 μohm cm	Dark Gold	0	100	0
S-005	Pre	4.26	30	60	16.22 ohm cm		0	100	0
S-011	Post	2.86	15	30	315.75 mohm cm	Clear	60	40	0
S-011	Pre	2.86	15	30	3.915 ohm cm		60	40	0
S-017	Post	0.43	7.5	15	332 mohm cm	Silver, semiclear	0	2	98
S-017	Pre	0.43	7.5	15	1.0425 mohm cm		0	2	98
S-025	Post	2.86	17	34	9.21 ohm cm	Clear	99	1	0
S-049	Post	2.86	20	40	147.4 mohm cm		97	3	0
S-002	Post	2.86	15	30	16.2 ohm cm	Clear	99	1	0
S-029	Pre	2.86	17	34	12.025 ohm cm		99	1	0
S-030	Post	2.86	34	68	736 mohm cm	light gold transp	22	78	0
S-031	Post	2.86	8	16	473 ohm cm	Clear	92	8	0
S-049	Pre	2.86	20	40	9.02 ohm cm		93	7	0
S-048	Pre	2.86	30	60	27.2 ohm cm		75	Less Than One	25
S-030	Pre	2.86	34	68	4.2 ohm cm		22	78	0
S-039	Pre	2.86	52	104	4.03 ohm cm		Low	High	None

Figure 10: Successfully measured samples, including resistivity only.

in the sample. The sample composition can be identified through this non-destructive technique. It is considered to be the most precise and accurate micro-analysis technique available for determining the elemental composition of the surface of materials [12].

For our thin films, EPMA can reach below our films and measure the composition of the substrate, so equivalent films were deposited onto pure silicon substrates. Glass (SiO_2) substrates creates a large background signal of oxygen in the sample, and while varying the excitation voltage can remove this error, it's simpler in this case to use a pure Si substrate. Our measurements were taken at CAMCOR at the University of Oregon, using a CAMECA SX50 Electron Microprobe. See figure 11 for data.

TiO2	Phase	pO2 (%)	Thickness (nm) Predicted	Pre A (EPMA) Thickness (nm)	Post A (EPMA) Thickness (nm)	Δ thickness	Ti PRE (at %)	O PRE (at %)	Ti POST (at%)	O POST (at %)
S-009-Si	?	0.43	30	32.9	34.2	1.3	0.474	0.526	0.452	0.548
S-010-Si	?	0.43	60	63.6	65.1	1.5	0.561	0.439	0.532	0.468
S-012-Si	?	2.86	30	25.8	27.3	1.5	0.347	0.653	0.337	0.664
S-022-Si	?	2.86	30	18.4	18.8	0.4	0.342	0.658	0.335	0.665
S-029-Si	?	2.86	34	21.83	15.4	-6.43	0.340	0.660	0.332	0.668
S-030-Si	Brookite	2.86	68	63.28	61.34	-1.94	0.355	0.645	0.349	0.652
S-030-Si	Rutile	2.86	68	63.28	61.4	-1.88	0.355	0.645	0.350	0.651
S-031-Si	?	2.86	16	16.71	17.8	1.09	0.3458	0.6542	0.3363	0.6637
S-032-Si	?	1.18	34	45.96	46.85	0.89	0.3761	0.6239	0.3578	0.6422
S-038-Si	?	2.86	8	2.91	3.39	0.48	0.3717	0.6283	0.34	0.65

Figure 11: EPMA samples measured.

5   Discussion

TiO_2 is considered fully oxygenated at an atomic percentage of 66% (2 out of 3 atoms are oxygen). Any percentage less than that indicates oxygen vacancies. For all samples measured, the oxygen atomic percentage was less than or equal to fully oxygenated. As can be seen on the graph of EPMA data, most of the samples were already highly oxygenated when measured. Despite this, oxygen content did increase after anneal – the line indicates where a sample would be considered unchanged on anneal. Annealing, despite being in a nitrogen flow environment, caused the samples to absorb oxygen. See figure12 for details.

When we discard highly oxygenated samples (samples with a pre-anneal oxygen content greater than 65%), we see a trend that indicates that lower oxygen content samples absorb more oxygen on anneal. This makes sense,
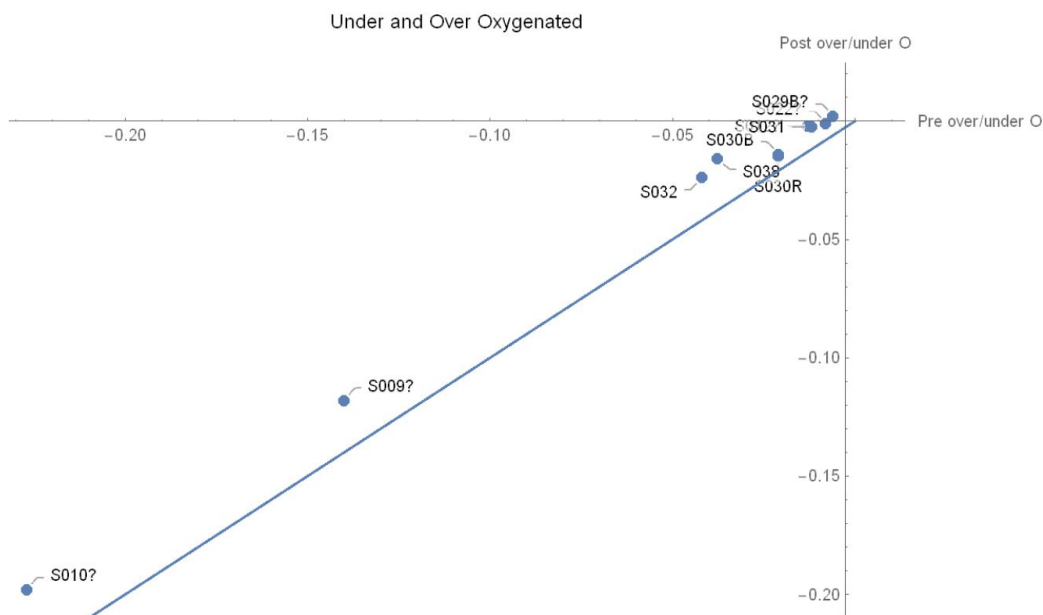
Figure 12: Oxygen content measured with EPMA - the line indicates points along which no change happens on anneal.

as less oxygenated samples contains more sites to accept a free oxygen. See figure 15 for details.

Unfortunately, we don't know the polymorph composition of these samples, which does not allow us to further distinguish between the absorption behaviour of different polymorphs, with the exception of sample 30. Sample 30 is a sample with a mixture of two polymorphs, about 22% brookite and 78% rutile. The brookite portion absorbed more oxygen proportionally than the rutile did. We cannot conclude anything specific from this one point, but it would be worthwhile to measure more samples this way, differentiating between recognizable polymorphs.

Sample 30's resistivity was 4.1 ohm cm, which was on the edge of what was measurable and did not allow us to measure carrier density as well. The
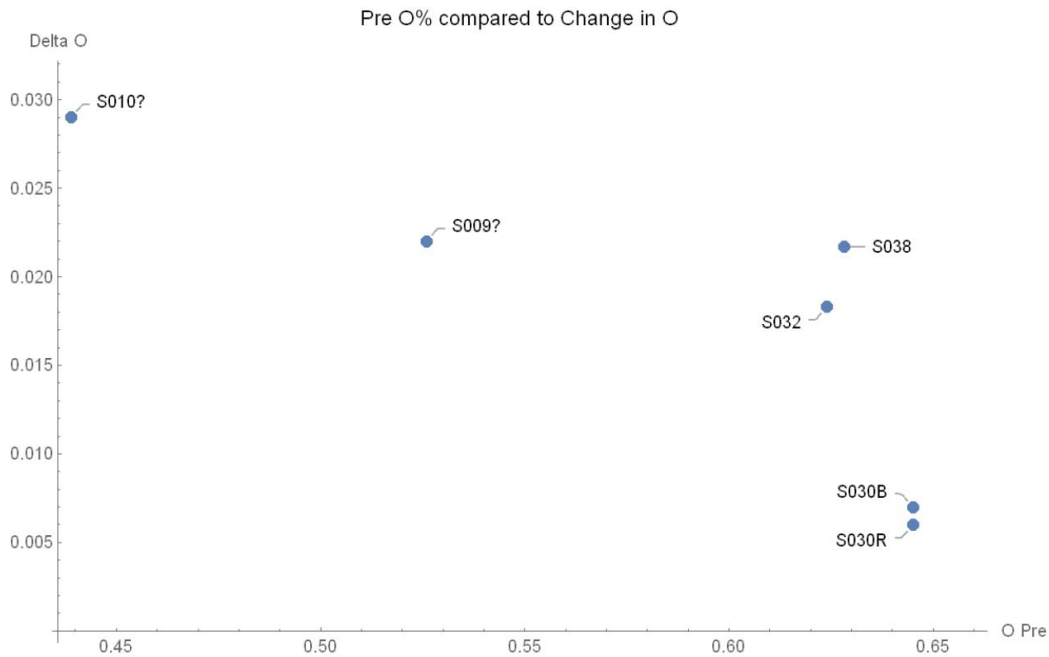
Figure 13: Change in oxygen content versus pre anneal oxygen content

other resistivities varied from 393 μohms cm to 16 ohms cm. When plotted against the oxygen percentage in the atmosphere during synthesis, we can't determine a pattern. See figure ??.

TiO2 is known to be an n-type semiconductor. Our measurement of S017, for example, shows that TiO2 is an n type, with a carrier density of $0.4 * 10^{20}$ cm^{-3}. This means that oxygen vacancies are the charge carriers for TiO2. Larger oxygen deficiencies mean more carriers, which correlates to better conductivity.

Without EPMA data, we can still perhaps estimate the oxygen content of the sample. Consider sample 30. On anneal, we would expect the oxygen content to increase, if the sample started out not fully oxygenated. This absorption of oxygen should cause the samples to increase in resistivity, but
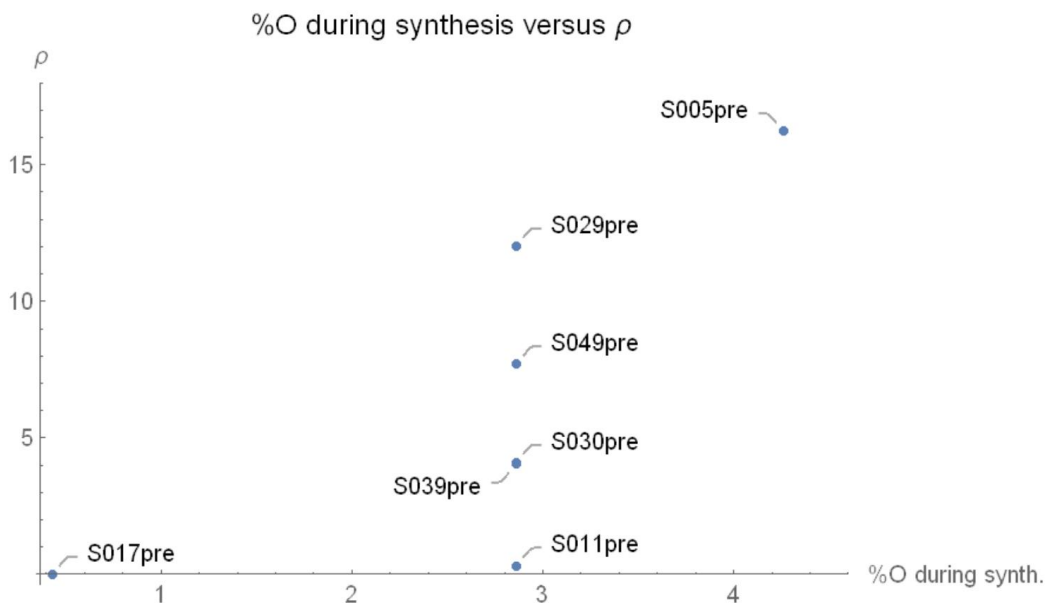
Figure 14: Resistivity versus oxygen content available during synthesis.

there are two extra factor to considers.

- Crystal Grain Boundaries: increase on anneal, increases resistivity

- Crystallization within a crystal: increase on anneal, decreases resistivity

- Oxygen Vacancies: decrease on anneal, increases resistivity

These three factors determine the resistivity of the sample. For fully oxygenated samples, the crystallization and crystal grain boundaries are the dominant factors, with crystallization within a grain boundary generally outweighing the increase in crystal grain boundaries. The mean free path decreases, and thus resistivity decreases. A sample that is not fully oxygenated, meanwhile, will have its resistivity increased by the decrease in oxygen vacancies. See figure 15
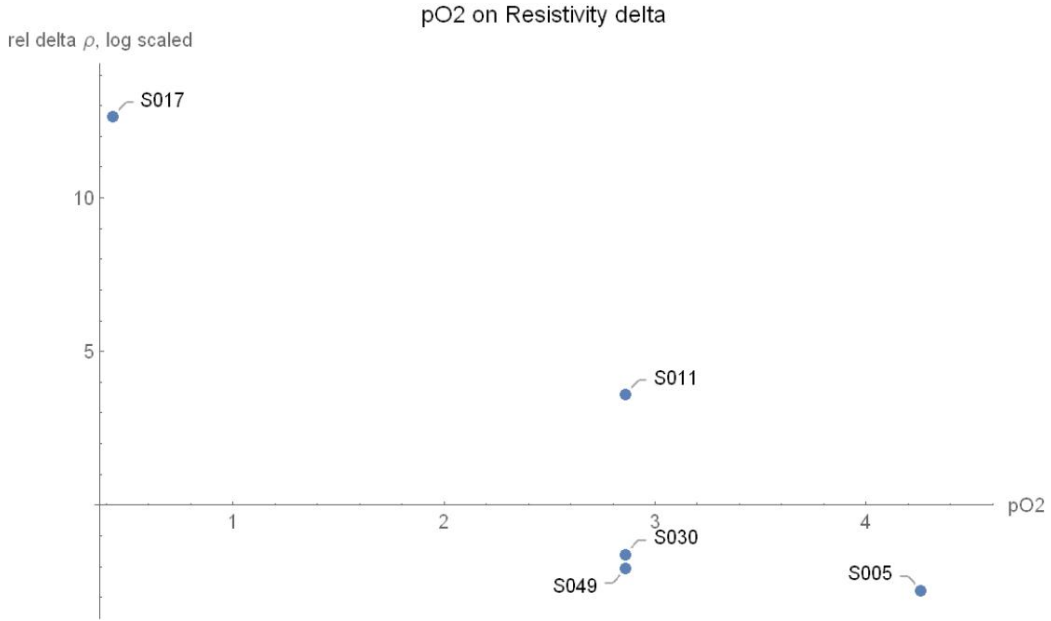
Figure 15: Change in resistivity versus oxygen present during synthesis

Considering sample 30, we can see the resistivity decreases on anneal. It has the smallest decrease of the three samples, which is due to its increase in oxygen (which was not dramatic, but still significant – see EPMA data). S049 and S005 both also decreased. Looking at their absolute resistivity on pre anneal, they were both above 4 ohm cm. I believe this is indicative of a nearly fully oxygenated sample. S017 and S011 both were not very resistive in the pre anneal measurements, and they became much more resistive.

We can therefore confirm that, given the resistivity measurements correlation with EPMA data, that TiO2 is an n-type semiconductor. Furthermore, the effects of crystallization will be swamped by the increase in oxygen content for samples less than about 4 ohm cm. However, in order to accurately measure the resistivity and carrier density of TiO2, we need resistivity to be less than about 400 mohm cm. This presents a problem, as pre and

post anneal measurements of resistivity will be distorted by the absorption of oxygen, even in a nitrogen flush.

For further work, samples will need to be produced which are underoxygenated, with resistivities of less than 400 mohm cm. As Brookite forms best at around a 2.86% oxygen environment, this presents a problem, as many samples produced began nearly full oxygenated, and only got worse with annealing. S011 was the only sample which we can reasonably expect to not be fully oxygenated, and it was only 60% brookite. For future work, some samples should be annealed in a vacuum oven if possible, to isolate the crystallization changes, and brookite will need to be synthesized at the lower edge of its oxygen needs – which fights for dominance with a more stable polymorph, rutile, which needs less oxygen to form. See figure 2.

Finally, considering the difficulty of synthesizing pure and oxygen deficient brookite, it may be necessary to extrapolate the resistivity of pure brookite from fractional brookite samples, taking into account the level of oxygen deficiencies we will expect from them.

~~J. Haggerty, L. Schelhas, D. Kitchaev, J. Mangum, L. Garten, W. Sun, K. Stone, J. Perkins, M. Toney, G. Ceder, D. Ginley, B. Gorman, J. Tate, "High-fraction brookite films from amorphous precursors", Scientific Reports, volume 7, Article number: 15232 (2017)~~

References

[1] J. Haggerty, L. Schelhas, D. Kitchaev, J. Mangum, L. Garten, W. Sun, K. Stone, J. Perkins, M. Toney, G. Ceder, D. Ginley, B. Gorman, J. Tate,

"High-fraction brookite films from amorphous precursors ", Scientific Reports, volume 7, ~~Article number:~~ 15232 (2017)

[2] J.Mangum, O. Agirseven, J. Haggerty, J. Perkins, L. Schelhas, D. Kitchaev, L. Garten, D. Ginley, M. Toney, J. Tate, B. Gorman, "Selective brookite polymorph formation related to the amorphous precursor state in TiO2 thin films", Journal of Non-Crystalline Solids, ~~Volume~~ 505, 1 February 2019, Pages 109-114

[3] M. K. Nowotny, T. Bak, J. Nowotny, "Electrical Properties and Defect Chemistry of TiO2 Single Crystal. I. Electrical Conductivity", J. Phys. Chem. B 2006, 110, 33, 16270-16282

[4] Kazuhito Hashimoto et al, "TiO2 Photocatalysis: A Historical Overview and Future Prospects", Jpn. J. Appl. Phys. 44 8269, 2005.

[5] D. Hanaor, C. Sorrell, "Review of the anatase to rutile phase transformation", Journal of Materials Science (2011) February 2011, Volume 46, ~~Issue 4,~~ pp 855–874. https://doi.org/10.1007/s10853-010-5113-0

[6] A. Di Paola, M. Bellardita, L. Palmisano, "Brookite, the least known TiO2 photocatalyst", Catalysts, 3, 2013.

[7] A.Weibel, R.Bouchet, P.Knauth, "Electrical properties and defect chemistry of anatase (TiO2)", Solid State Ionics, Volume 177, Issues 3–4, 31 January 2006, Pages 229-236

[8] A. Folger, J. Kalb, L. Schmidt-Mende, C. Scheu, "Tuning the Electronic Conductivity in Hydrothermally Grown Rutile TiO2 Nanowires: Effect

of Heat Treatment in Different Environments", Nanomaterials (Basel). 2017 Oct; 7(10): 289.

[9] N. Ghenzi, M. J. Rozenberg, R. Llopis, P. Levy, L. E. Hueso, and P. Stolia, "Tuning the resistive switching properties of TiO2-x films", Appl. Phys. Lett. 106, 123509 (2015)

[10] L.J. Van der Pauw, "A method of measuring specific resistivity and Hall effect of discs of arbitrary shape", Philips Research Reports. 13: 1–9, 1958.

[11] National Institute of Standards and Technology, "Resistivity and Hall Measurements", https://www.nist.gov/pml/engineering-physics-division/popular-links/hall-effect/resistivity-and-hall-measurements, updated 2018.

[12] Cameca, "Introduction to EPMA", https://www.cameca.com/products/epma/technique